Chapter 4. Conserved prolines in the M2-M3 loop

4.1 Introduction

Ligand-gated ion channels (LGIC) are highly dynamic proteins, undergoing multiple conformational transitions among various states. Their primary function is to transduce a chemical signal— binding of a small molecule— into an electrical signal— ion flux across the cell membrane. They accomplish this feat through a global reorganization of their quaternary structure. Agonist binding to these proteins initiates a series of conformational changes resulting in the opening of an ion permeant channel across the cell membrane. This process, linking agonist binding to the open conductance state of the receptor, is termed gating.[1-3] From a molecular perspective, this represents a fairly amazing process. The agonist-binding site and channel gate are separated by almost 50 Å and nearly 100 amino acids of the protein's primary sequence. Thus, the number of steric and noncovalent interactions driving this conformational transition is significantly greater than that traditionally considered in the conformational analysis of organic molecules. Although advances in areas such as molecular dynamics have certainly broadened the theoretical framework necessary for conformational analysis on this scale, molecular details of the gating process still remain poorly understood.

Study of the gating process in LGICs has lacked an essential ingredient: structural information. This has made it difficult to relate functional changes observed in structure-function studies to specific structural transitions associated with the gating process. However, with recent publications of the AChBP crystal structures[4, 5] and Nigel Unwin's structure of the transmembrane domains derived from 4 Å cryo-electron micrographs

(cryo-EM) of the *Torpedo* nAChR,[6] we may finally have sufficient structural information to elucidate some of the molecular events of the gating mechanism.

Presumably, local conformational changes at the binding site (arising from agonist binding) initiate the gating mechanism. It is believed that rather than communicating these changes sequentially through the primary sequence of the protein, intermediate functional domains link binding site changes to the receptor gate.[7] Evidence from several studies highlights the possibility that the functional interface between the extracellular and transmembrane domains is formed by interacting loops contributed by each domain. Both biophysical studies and structural data point to two loops: the Cys loop and β1-β2 loop in the extracellular domain as important components of the gating pathway.[6, 8] In a recent study where chimeric receptors were constructed by replacing the extracellular domain of the 5-HT_3R with the AChBP sequence, functional receptors were observed only in chimeras where both the Cys loop and the β1-β2 loop contained the 5-HT_3R amino acid sequence.[9] This work provides telling evidence that these loops may form functional domains, coupling conformational changes at the binding site to the channel gate.

Findings from several studies indicate that the Cys and β1-β2 loops convey structural changes in the extracellular domain to the channel gate through a direct interaction with the M2-M3 loop— a short loop that connects transmembrane domains M2 and M3 and projects above the extracellular membrane.[2, 6, 8-10] The M2-M3 loop is an appealing candidate because not only are there several studies supporting its involvement in the gating process (discussed below), but the channel gate lies in M2. Hence any movement of M2 would likely involve conformational changes in this loop. In the work

presented in this chapter, nonsense suppression methodology is used to investigate the functional role of two conserved prolines, 301 and 308, in the M2-M3 loop of the 5-HT_3R. This work has been a collaborative effort with the Sarah Lummis group at the University of Cambridge . Sarah Lummis performed all of the immunofluorescence work and contributed significant effort to the electrophysiology experiments.

4.2 Transmembrane domains and the M2-M3 loop

As detailed in chapter 1, LGICs are formed by five subunits arranged in a pentagonal array around a central pore. Each subunit has four transmembrane domains as identified by hydropathy analysis. The cryo-EM structure of the transmembrane region shows that each of these domains forms an α-helix spanning the bilayer[6] (Figure 4.1). The M2 domain of each subunit lines the channel lumen with the side chains of Leu 9' and Val 13' in M2 (the convention for numbering residues in M2 starts with 1' at the N-terminal or cytoplasmic side), forming the channel gate. These are thought to present a hydrophobic barrier preventing the flow of ions.[11] The overall structure detailed by the cryo-EM images is supported by much of the previous biochemical and electrophysiological work. Indeed, several earlier studies proposed an α-helical structure for M2[12, 13], and Leu 9' has long been thought to form the channel gate.[14, 15] In addition, several novel features predicted by the structure have also been suggested by earlier work. In Unwin's structure, the M2 helix extends two turns above the membrane. Results from $GABA_A$ studies using the substituted cystine accessibility method (SCAM) showed a modification pattern consistent with an extended helix.[16] The structure also shows a water-filled crevice between M2 and M3 which previously had been suggested.[17]

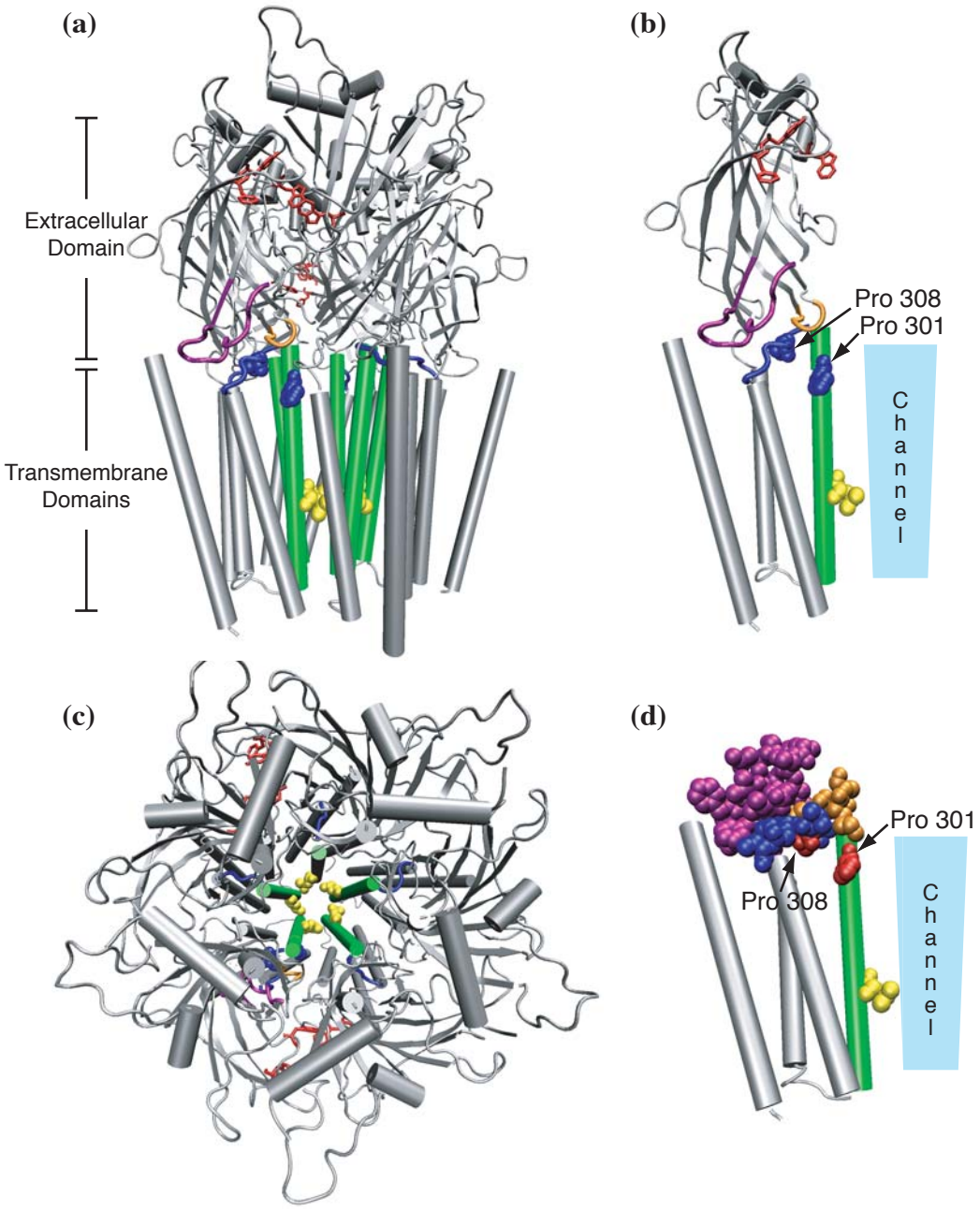

Figure 4.1. Several views of the 5-HT_3R as predicted by homology modeling. Highlighted features: binding site (red), Cys loop (purple), β1-β2 loop (orange), M2 (green), M2-M3 loop (blue), Leu 9' (yellow) and prolines 301 and 308 (blue CPK in *a-c* and red CPK in *d*). (a) Side view of entire receptor showing general arrangement of extracellular and transmembrane domains. (b) Single subunit showing Pro 301 and 308, and transmembrane topology. (c) Top view looking down the pore from the extracellular side. The cluster of residues (Leu 9') forms the channel gate. (d) Transmembrane domains, Cys loop and β1-β2 loop of a single subunit showing relative location of the loop structures.

Based on the cryo-EM data Unwin has proposed a model for the gating mechanism in nAChR (and by extension all LGIC).[6] The model posits that ligand binding induces a 15° rotation of the α subunits, which in turn, causes the tip of the β1-β2 loop— Val 44 specifically— to contact the M2-M3 loop (docking into the hydrophobic pocket formed by Ser 269-Pro 272 of the M2-M3 loop). The torsional force provided by this contact pivots the M2-M3 loop, thereby rotating M2 and gating the receptor. Although this seems to be a plausible model for the gating process, as yet, there is still a lack of experimental evidence to substantiate it. Several of the details, however, are supported by previous findings.

In the model, the M2-M3 loop plays a prominent role in the gating process. It not only serves as the direct link communicating conformational changes in the extracellular domain to the channel gate, but also functions as a pivot point for the gating movement of M2. The M2-M3 loop has long been speculated to be part of the gating pathway. Mutagenesis studies in the GlyR and nAChR showed that mutations in this loop could decouple agonist binding and channel gating.[18-22] More detailed single-channel studies in the nAChR demonstrated that mutations in the M2-M3 loop affect the gating equilibrium and do not change the binding equilibrium.[23] These studies also showed that the effects of mutations in the loop were dependent on their position in the primary sequence of the loop with one mutation increasing the gating rate and a similar substitution at the adjacent residue decreasing the rate. SCAM studies in both the GlyR and $GABA_A$ have shown the M2-M3 loop becomes more water accessible during channel gating, indicating that it undergoes a conformational change during the process.[16, 24]

A recent study in $GABA_A$ points to a direct interaction between the M2-M3 loop and the Cys loop during the gating process.[8] This study swapped charged residues between the Cys and M2-M3 loops to show that an electrostatic interaction between a Lys in the M2-M3 loop and a conserved Asp in the Cys loop is formed during gating. Interestingly, this Lys is not conserved in either the nAChR or 5-HT_3R, and similar studies in the GlyR did not show the same interaction[10]— raising the possibility that there may be subtle variations in the gating mechanism for each of the Cys-loop receptors. Unwin's model emphasizes an interaction between the β1-β2 loop and M2-M3. It is very likely that M2-M3 interacts with both of these extracellular loops. Inspection of the structure in Figure 4.1d shows that the Cys and β1-β2 loops bracket M2-M3, and the chimeric studies point to a need for both loops in coupling agonist binding and channel gating. Thus, while the exact role the M2-M3 loop plays is not clear, the cumulative evidence strongly supports it being functionally important in the gating pathway.

4.3 Potential dynamic role of proline

One interesting feature of the M2-M3 loop in the 5-HT_3R is the presence of two proline residues (Figure 4.2). Pro 301 is conserved in all Cys-loop receptors and is located roughly two helical turns below the C-terminal end of M2 (Figure 4.1). Pro 308 is conserved in all of the cation-selective receptors (nAChR and 5-HT_3R) and is located two residues after the C-terminal end of the extended M2 helix (Figure 4.1). This proline aligns with Pro 272 in the nAChR, which in Unwin's model forms part of the hydrophobic pocket into which the β1- β2 loop docks. Proline has several special features (discussed below) that make it an intriguing consideration in terms of the gating process.

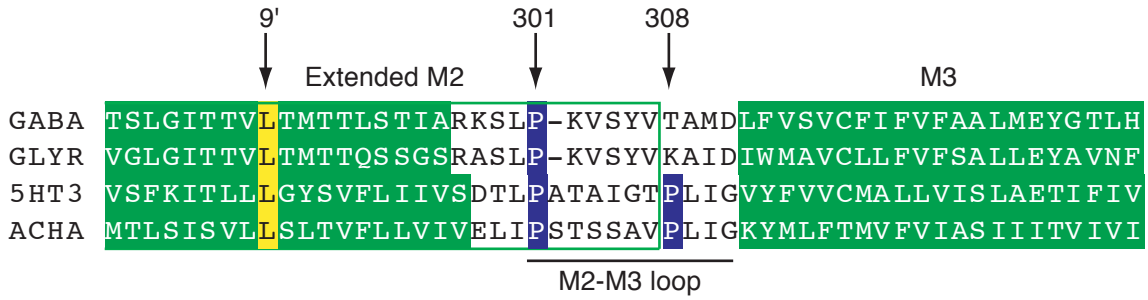

Figure 4.2. Sequence alignment of the murine sequences for α_1 $GABA_A$, α_1 GlyR, 5-HT_{3A}R, and α_1 nAChR. Pro 301, Pro 308, and secondary structural domains are indicated. The M2 helix as identified by hydropathy analysis is shown in green, and the extended helix as predicted in the cryo-EM structure is designated by the green box. Pro 301 is conserved in all Cys loop receptors, Pro 308 is conserved in the cation-selective receptors.

Proline is unique among the 20 standard amino acids in that its side chain is covalently bonded to the α-amino group. This cyclic structure severely limits the main chain conformations proline can adopt. In terms of the backbone dihedral angles, ϕ and ψ, proline is the most conformationally restricted amino acid. The cyclic structure fixes the ϕ dihedral at -65°±25° and leaves the ψ dihedral hindered with two local minima near –55° and 145°, though surveys of the protein databank show that ψ values around 80° are also common.[25, 26] Another consequence of the cyclic structure is that the secondary peptide bond formed with the nitrogen of proline lacks a hydrogen, resulting in the loss of a hydrogen-bond donor at prolyl backbone sites. Due to its conformational limitations and the absence of an amide hydrogen, proline is rarely found in periodic secondary structure such as β-sheets or α-helices.[25, 26] In fact, in globular proteins, proline is considered the classic helix-breaker.

Interestingly proline is found with anomalous frequency in the putative helices of integral membrane receptors and transport proteins.[27] The reasons for this are not yet clear, but it has lead to wide speculation that proline is important in the structure and

function of these proteins.[28-30] The potential importance of proline is evidenced by the recent observation that mutations of proline have one of the highest phenotypic propensities in the analysis of TM sequences from the Human Gene Mutation Database.[31] As a result of its lacking a hydrogen-bond donor and the local steric restrictions it presents, proline, when found in helices imparts a 25º kink to the helix trajectory.[32, 33] From a structural standpoint, modeling studies have shown that this kink can serve to stabilize transmembrane helix bundles by increasing the van der Waals contact between the helices.[34] It is also hypothesized that a proline kink may serve a dynamic role because it removes at least one hydrogen-bonding pair (between the NH of proline at *i* and the carbonyl O at *i-4*) and often leads to loss of a second pair (the NH of *i+1* and the carbonyl O of *i-3*).[28, 29] This allows the two ends of the helix to pivot independently. Thus, the proline kink could function as a hinge point in the conformational changes of ion channel function.

Another interesting feature that has generated much speculation about proline is it is the only standard amino acid for which the *cis* peptide bond is energetically accessible[30] (Figure 4.3). Surveys of the protein data bank show that roughly 5-6% of all prolines are in the *cis* conformation, as opposed to the other amino acids for which less than 1% are *cis*.[35, 36] Proline's ability to adopt the *cis* conformation arises largely due to destabilization of the *trans* conformation from steric conflicts between C_δ of proline and C_β of the preceding residue. From a structural standpoint, *cis* proline is found in several types of β-turns, where the protein chain direction is reversed over a short distance.[26, 37] This characteristic of proline may also play a dynamic role in that *cis*/*trans* isomerization of prolyl peptide bonds may function as a conformational switch.[38] Recently, several

cis/*trans* proline switches have been elucidated in globular proteins, most notably the tyrosine kinase Itk where isomerization shuttles the protein between different active states.[39-41]

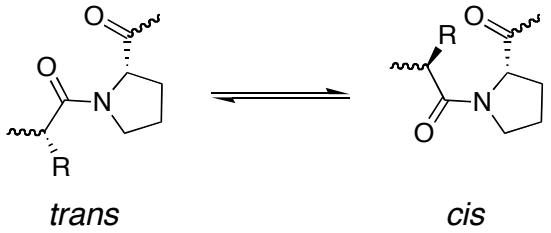

Figure 4.3. Schematic of *trans* and *cis* conformations of the prolyl peptide bond.

It has long been speculated that *cis*/*trans* isomerization of prolyl peptide bonds could be involved in the gating pathway of ion channels.[27, 30] Indirect evidence has come from studies on gap junction proteins[42], but to date, there is no clear experimental evidence supporting this hypothesis. However, given the anomalous frequency of proline in transmembrane helices and the recent demonstrations of proline switches, this still remains an attractive hypothesis. Another potential way in which proline could facilitate the conformational changes associated with ion channel gating is in shuttling between favored states at the hindered ψ angle. NMR studies on model peptides corresponding to the second intracellular loop of the vasopressin receptor (a GPCR) have demonstrated a conformationally heterogeneous proline, where the ψ angle flipped between two stable conformations.[43] This proline is conserved throughout the GPCR family and is believed to be important for coupling to G proteins. Thus, this may represent a general motif where proline functions as a conformational switch without *cis*/*trans* isomerization.

4.4 Experimental design

A series of proline analogs was selected to evaluate the functional role of Pro 301 and Pro 308 in the 5-HT_3R (Figure 4.4). The analogs were chosen to assay specific features of proline's structure and function, and many of the analogs have been previously studied in model peptides, providing some quantitative background data for interpreting our results.[44-50] In addition some of the analogs have been used in previous nonsense suppression studies to evaluate a conserved proline in the M1 domain of the nAChR and 5-HT_3R.[51, 52]

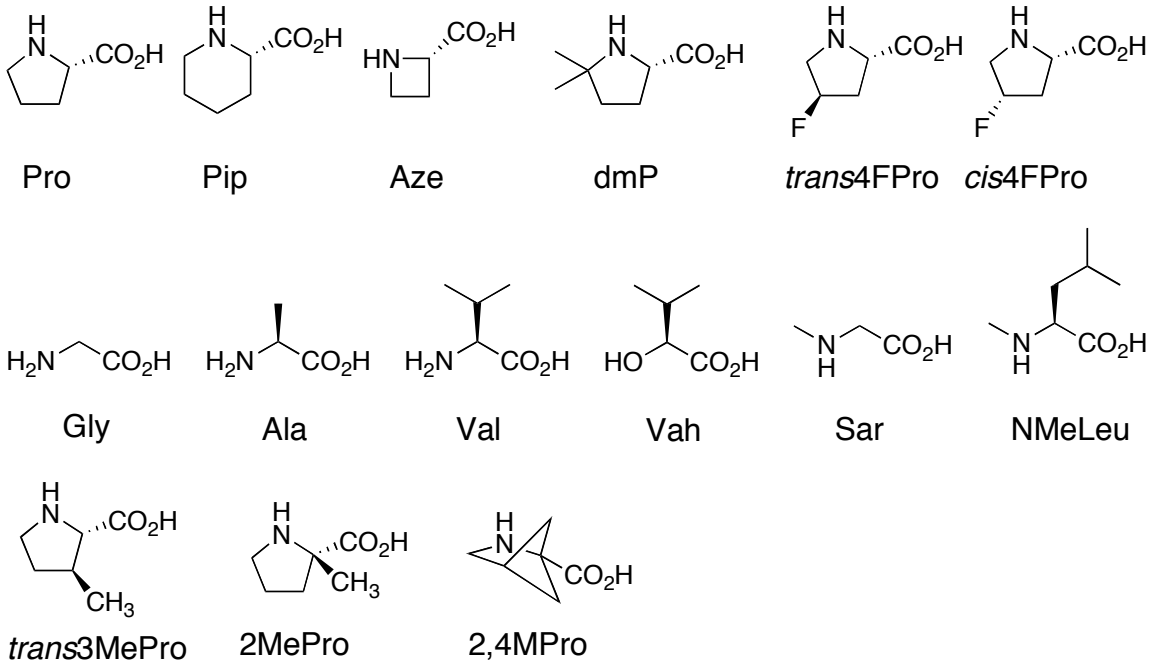

Figure 4.4. Structures of the amino acids used to probe Pro 308 and Pro 301.

In many ways, proline is an ideal target residue for structure-function studies with unnatural amino acids, as it has several features that can be readily tested with minor perturbations. Ring size and the attendant flexibility can be tested with the 4- and 6-membered ring analogs, Aze and Pip, respectively. The ring of proline displays two

stable conformations: endo pucker and exo pucker (discussed below). This feature of proline can be tested with the fluoro-prolines, which each prefer a different puckered conformation.[47, 53] The hydrogen bonding properties can be examined using backbone ester substitutions with hydroxy acids or N-methyl amino acids.[51] The latter can also be used to assay the potential role of the secondary prolyl amide. In addition N-methyl amino acids mirror many of the conformational features of proline, but lack the rigid ring structure. Finally the potential of *cis*/*trans* isomerization can be readily tested using analogs of proline that are selective for a particular conformation (*cis*-selective: Aze, Pip, and dmP[46, 48]; *trans*-selective: *trans*-3-Me-Pro, 2-Me-Pro, and 2,4-methano-Pro[44, 49, 54]).

4.5 Results

4.5.1 General experimental details

Both unnatural and natural amino acids were incorporated into positions 301 and 308 of the 5-HT_3R using *in vivo* nonsense suppression methods, and mutant receptors were evaluated electrophysiologically[55]. The whole-cell currents induced by the application of 5-HT were measured by two-electrode voltage clamp techniques. Non-functional receptors were assayed for surface expression using immunofluorescent imaging. The functional effects arising from the introduced mutations were determined from the dose-response relations and the macroscopic rate constants for receptor activation and deactivation. Macroscopic rate constants were determined from the single-exponential fits of the whole-cell current traces using *pCLAMP 9.0* analysis software. In all experiments, the 5-HT_{3A}R homomer was used.

4.5.2 Control experiments for 301 and 308

Initial experiments at both 301 and 308 focused on several important controls: ensuring no protein was produced through any read-through of the UAG-containing mRNA, and recovery of the wild type receptor through nonsense suppression. Injection of either of mRNA with the UAG stop codon at 301 or 308 resulted in no 5-HT induced currents. In addition, injection of UAG-containing mRNA and uncharged tRNA produced no 5-HT induced currents at either site. Both of these controls indicate that in the absence of charged tRNA functional receptors are not produced by read-through of the UAG-containing mRNA. Injection of UAG-modified mRNA with aminoacyl tRNA-Pro into oocytes resulted in receptors with functional properties similar to wild type, EC_{50}s of ~1.2 μM and Hill coefficients of ~2 (Table 4.1 and 4.2).

4.1.3 Electrophysiology results for substitution at 308

4.1.3.1 Dose-response data

In all, 15 different residues were attempted at position 308. Interestingly, nine of these did not produce functional receptors (see Table 4.1), indicating this is a fairly stringent position. All mutations that produced functional receptors were close analogs of proline and maintained a cyclic structure. The dose-response data show that with the exception of dmP, the functional mutations lead to only modest changes in EC_{50} (Figure 4.5 and Table 4.1). The two ring-size analogs, Aze and Pip, lead to 3- and 1.7-fold reductions in EC_{50}, respectively, whereas the two fluoro-prolines, *cis*-4-F-Pro and *trans*-4-F-Pro, produced EC_{50}s very near wild type. In the case of dmP, however, a 23-fold reduction in EC_{50} was observed. This finding is suggestive of the possibility that

a *cis*-proline is functionally important at position 308, as model peptide studies have shown dmP to prefer the *cis*-amide isomer by ~1.1 kcal/mol relative to *trans*.[48] It is also possible that given the increased sterics of dmP, this residue alters the conformation of the M2-M3 loop, biasing it towards the open state conformation.

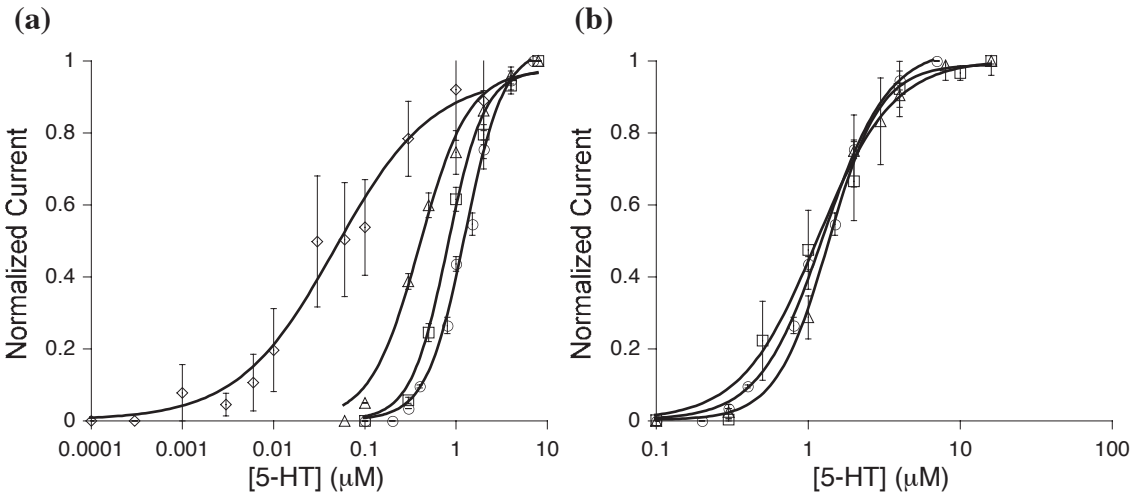

Figure 4.5. Dose-response relations for Pro 308 mutants. (a) Pro (*circles*), Aze (*triangles*), Pip (*squares*), and dmP (*diamonds*). (b) Pro (*circles*), *cis*-4-F-Pro (*squares*), and *trans*-4-F-Pro (*triangles*).

Further analysis of the dose-response data shows a strong correlation between the EC_{50} for the mutant receptors and the *cis* preference of the proline analogs (Table 4.2). Figure 4.6 shows a plot of $\Delta\Delta G$ EC_{50} (mutant – wt) versus $\Delta\Delta G$ for the cis preference of the analogs relative to proline. The linear correlation seen for the plotted values provides additional evidence that a *cis* proline at 308 may be functionally important in the gating mechanism.

Several underlying assumptions in this plot, however, should be noted. The quantity EC_{50} is not a true equilibrium constant. It is a composite of equilibria for both binding and gating. Our assumption, however, is that changes in EC_{50} with these mutants

reflect changes in the gating equilibrium and do not affect binding. Support for this assumption comes from single-channel studies which demonstrated that mutations in this region of the nAChR solely affected gating.[23] Furthermore, position 308 is ~30 Å from the binding site, and thus, mutations here are not likely to affect agonist binding. The $\Delta\Delta G$ values for the *cis* preference of the analogs come from several literature studies and were determined for small model peptides.[46-48] It is known that many factors including both the local protein sequence and longer-range interactions can affect the *cis* preference of proline.[36, 37, 56] We assume, however, that these factors will be similar for all the analogs considered, and thus, the trend in *cis* preference for the analogs will not be overly distorted from that seen in the model studies. Finally, this plot, although spanning two orders of magnitude in EC_{50}, shows that the data is clustered into two regions. The plot requires an intermediate data point between Aze and dmP, as linear fits of data clustered into two regions can be misleading.

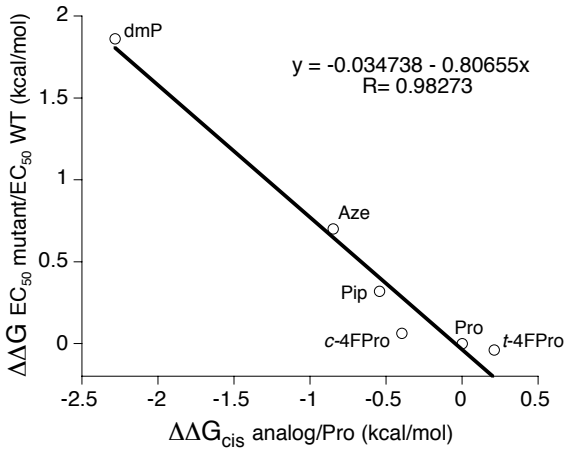

Figure 4.6. Plot of ΔΔG EC_{50} for the Pro 308 mutants versus ΔΔG for the *cis* preference of the analogs relative to proline. Equation for the linear fit and R value are shown at the top.

Table 4.1 Dose-response data and macroscopic rates for the Pro 308 mutants

Residue	EC_{50}±SEM (μM)	Hill±SEM	Act. rate±SEM (s^{-1})	Deact. Rate±SEM (s^{-1})
Pro	1.29 ± 0.07	2.04 ± 0.18	2.85 ± 0.91	0.03 ± 0.01
Aze	0.42 ± 0.03	1.56 ± 0.19	0.48 ± 0.06	0.02 ± 0.01
Pip	0.75 ± 0.06	2.16 ± 0.28	8.61 ± 0.27	0.29 ± 0.03
*cis*4FPro	1.16 ± 0.12	1.74 ± 0.27	5.95 ± 0.75	ND
*trans*4FPro	1.38 ± 0.06	2.53 ± 0.23	7.22 ± 0.34	ND
dmP	0.055 ± 0.01	0.77 ± 0.1	2.93 ± 0.69	ND
Ala	NR	NR		
Gly	NR	NR		
Val	NR	NR		
Vah	NR	NR		
Sar	NR	NR		
NMeLeu	NR	NR		
*trans*3MePro	NR	NR		
2,4MPro	NR	NR		
2MePro	NR	NR		

ND = not attempted, NR = no response to concentrations up to 1 mM 5-HT

Table 4.2. Thermodynamic data for proline analogs

Residue	*%cis*	K_{cis}	ΔG_{cis} (kcal/mol)	$\Delta\Delta G_{cis}$[a] (kcal/mol)
Reference 47				
Pro	17	0.20	0.96	0.0
*trans*4FPro	12	0.14	1.17	0.21
*cis*4FPro	28	0.39	0.55	-0.40
Reference 46				
Pro	6	0.06	1.67	0.0
Pip	13	0.15	1.13	-0.54
Aze	20	0.25	0.82	-0.85
Reference 48				
Pro	13	0.15	1.13	0.0
dmP	87.5	7.0	-1.15	-2.28

[a] ΔΔGcis for analog/proline

4.1.1.2 Incorporation of dmP at 308 shows blockable leak currents

Experimental support for the conclusion that the dmP 308 mutant stabilizes the open channel conformation of the M2-M3 loop comes from the observation that oocytes expressing dmP-containing receptors showed a continual increase in leak current following initial receptor activation (Figure 4.7). This leak was almost completely reversible by the open-channel blocker TMB-8, indicating the leak current was associated with receptor activation and not with any oocyte specific process. This finding suggests that upon activation dmP locks the channel in the open state. Furthermore, the lowered EC_{50} and blockable leak current seen with the dmP mutant indicate that Pro 308 undergoes a conformational change associated with the gating pathway.

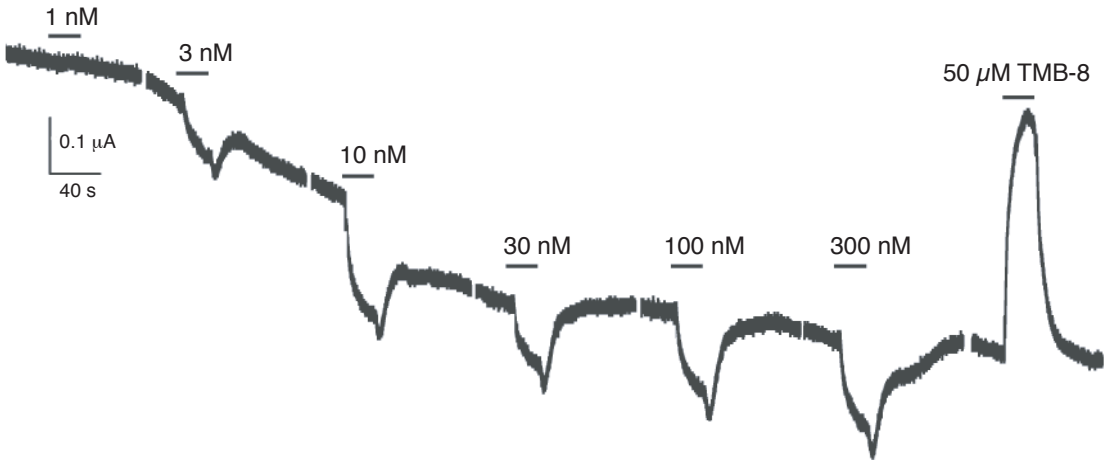

Figure 4.7. Current traces for dmP at position 308, showing the TMB-8 blockable leak currents seen after receptor activation by 5-HT. Bars represent 5-HT application.

4.1.1.3 Macroscopic rates

An interesting feature of these studies is that all functional mutants at 308 lead to changes in the macroscopic rates of activation and desensitization (Table 4.1). Figure 4.8 shows representative traces illustrating the altered rates. The fluoro-prolines and dmP lead to ~2-fold increases in the macroscopic activation rates. Pip lead to 3- and 8-fold increases in the rates of activation and deactivation, respectively. Aze was the only mutation to show decreased rates, producing a 6- and 1.7-fold decrease in activation and deactivation, respectively.

The rates for Aze, Pro and Pip match the trend in ring size with the 4-membered ring (Aze) slower than the 5 (Pro) and 5-membered ring slower than the 6 (Pip). It is possible that this trend in rates reflects differences in either ring flexibility or ring conformation among these residues. The potential importance of the ring conformation is supported by the changes seen with the fluoro-prolines, as *cis*-4-F-Pro favors an endo ring pucker and *trans*-4-F-Pro favors an exo ring pucker (Figure 4.9).[47, 53, 57, 58] (The

proline ring exhibits two preferred ring conformations or puckers: endo where C_γ is flipped *cis* to the carboxy group and exo where C_γ is flipped *trans* to the carboxy group). Thus, small changes in the ring conformation may cause subtle differences in the gating pathway.

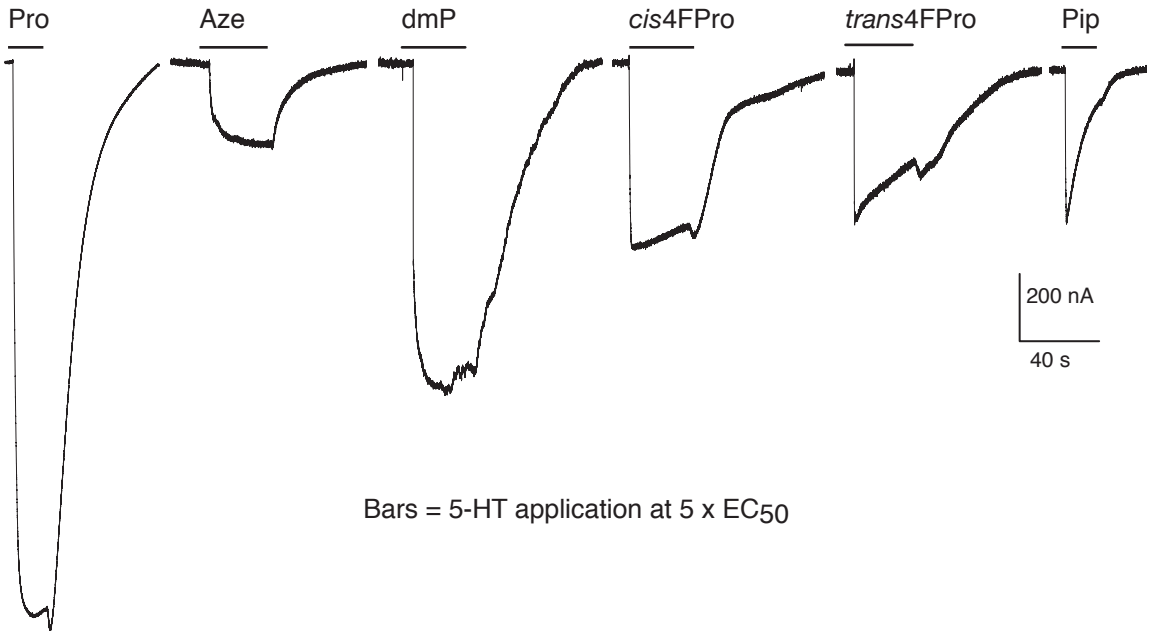

Figure 4.8. Current traces showing the altered rates of activation and deactivation for the 308 mutants. Bars represent application of 5-HT at 5 times EC_{50} of the respective mutant.

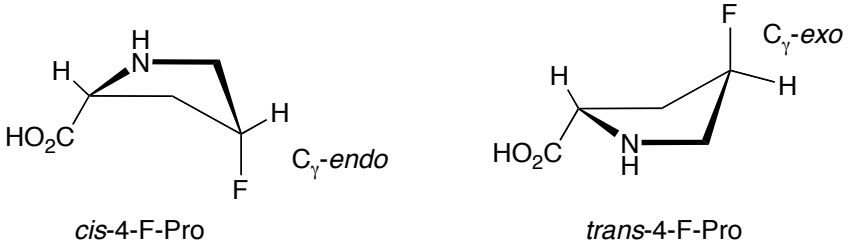

Figure 4.9. Schematic showing the two stable ring conformations (endo and exo) in proline and the preferred ring conformation for the 4-fluoro prolines.

4.1.4 Surface expression of nonfunctional mutants at 308

In order to rule out the possibility that the nonfunctional mutants arose from injection of hydrolyzed aminoacyl-tRNA, all tRNAs were analyzed by MALDI-TOF mass spec to ensure that the aminoacyl linkage was still intact.[59] In addition, all the attempted residues have successfully been incorporated into other sites in either the 5-HT_3R or nAChR using nonsense suppression.[51, 52] Thus, it seems very doubtful that the lack of functional receptors was caused by any incompatibilities with the ribosome or translation machinery.

The cell-surface expression of the non-functional mutants was examined by immunofluorescence to determine if these mutations had impaired receptor assembly and processing, or if they produced surfaced expressed but silent receptors. This work was performed by Sarah Lummis. Oocytes expressing the mutant receptors were fixed in 4 % paraformaldehyde, placed in glycerol and strored at –80º C. After thawing, oocytes were labeled with the primary antibody pAB120, washed, and then labeled with the secondary antibody, Cy5-conjugated anti-rabbit IgG.[60] Immunofluorescence was observed with a Nikon optiphot or a confocal (BioRad-MRC600) microscope.

All of the nonfunctional mutants showed surface labeling, indicating that these mutations had lead to silent receptors (Figure 4.10). The fact that the natural amino acids Gly, Ala, and Val produced surface expressed but silent receptors supports the idea that this position requires a conformationally restricted residue. However, even the N-methyl amino acids Sar and N-Me-Leu were silent, and as these residues replicate some of the conformational restrictions imposed by proline but lack the ring, clearly the more rigid ring structure is important. The fact that both the N-methyl residues and Vah were silent

rules out the possibility that the unique hydrogen bonding characteristics of Pro 308 are important. This latter possibility was found to be the case in earlier studies of a conserved proline in M1 of both the nAChR and 5-HT_3R.[51, 52] These studies found that replacement of this proline with a hydroxy acid produced functional receptors with wild type characteristics.

Not all of the ring-containing residues produced functional receptors. 2-Me-Pro, *trans*-3-Me-Pro and 2,4-methano-Pro were all silent. This suggests that the rigid ring structure is not sufficient to produce functional receptors. Both 2-Me-Pro and 2,4-methano-Pro are highly selective for the *trans* amide bond, lending further support to the possibility of a functionally important *cis* peptide bond at position 308.[49, 54] *Trans*-3-Me-Pro, on the other hand, is a fairly close analog of proline and studies have shown that it closely mirrors proline's *cis* preference.[49] One difference for *trans*-3-Me-Pro is that it has a higher barrier to *cis*/*trans* isomerization.[26, 44] This supports the conclusion that *cis*/*trans* isomerization at Pro 308 is mechanistically important in the gating pathway. Additionally, the reason for the higher barrier in *trans*-3-Me-Pro is believed to arise from its inability to form a hydrogen bond between the prolyl N and the NH at position *i+1*. This hydrogen bond has been shown to catalyze isomerization of prolyl-peptide bonds, increasing the isomerization rate 260-fold in model studies.[61, 62] One of the concerns for suggesting *cis*/*trans* isomerization at Pro 308 is that this isomerization may proceed at too slow a rate to be functionally viable in receptor gating, as the latter process occurs on the μs to ms timescale and isomerization is more often on the *seconds* timescale. Thus, the results with *trans*-3-Me-Pro point to the possibility that the formation of this hydrogen bond may catalyze the isomerization at Pro 308. It should also be noted that many

researchers have hypothesized that long-range protein interactions could increase the isomerization rate of proline, to make it a viable conformational switch in fast-acting processes.[30, 56]

Aside from the trends in *cis* and *trans* preference, the immunofluorescence findings show that incorporation of proline analogs substituted at the 2 or 3 position results in receptors where agonist binding and channel gating have been decoupled. A possible explanation is that steric bulk on this side of the proline ring may disrupt the proper orientation of the M2-M3 loop. Alternatively, bulk on this side of the ring may interfere with specific interactions of the proline ring, possibly even with interactions between Pro 308 and one of the extracellular loops. This latter speculation could fit with Unwin's model in that steric bulk at the 2 or 3 position of the proline ring may prevent docking of the β1- β2 loop into the hydrophobic pocket of the M2-M3 loop.

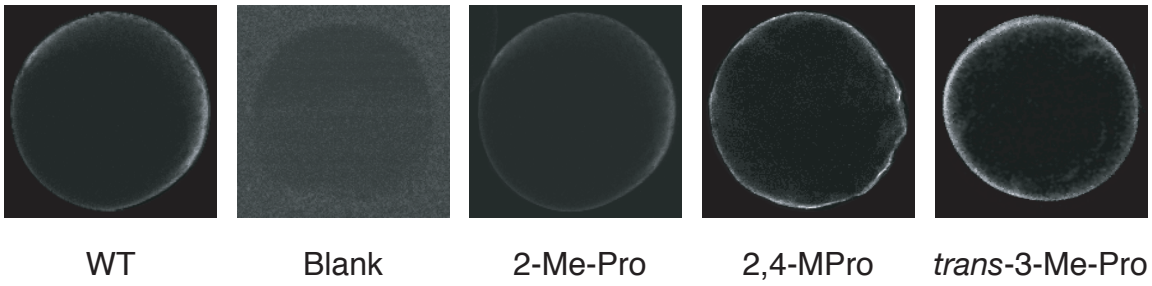

Figure 4.10. Immunofluorescent images of the nonfunctional 308 mutants. Visible labeling of mutants expressing *trans*-selective proline analogs demonstrates these receptors are expressed at the cell surface.

4.1.5 Poor expression of dmP and Aze at 308

A final observation to note in the studies of Pro 308 is that both dmP and Aze displayed very inconsistent expression. In all, approximately 200 oocytes from 10 different batches were tried for each of the residues. For dmP, expression was seen in

only 9 oocytes and with Aze, 13 oocytes showed expression. Several avenues were taken to increase the expression in these two mutants: incubation at different temperatures, expression with the 5-HT_{3B} subunit, and double injection. None, however, lead to any increase in expression.

Both of these unnaturals present steric and conformational demands. In dmP significant steric bulk has been introduced adjacent to the nitrogen. This may interfere with the efficiency of the peptidyl-transfer reaction during translation. In Aze, the conformational restrictions imposed by the 4-membered ring may interfere with processing and assembly. This latter concern could also be a problem with dmP mutants. It is known that the folding of the 5-HT_3R is dependent on the activity of the proline-peptidyl isomerase cyclophilin A (CypA).[63] It is plausible that dmP and Aze are inefficient substrates for CypA, which would certainly lead to a reduction in the expression for both mutants. In addition, studies of the cystic fibrosis transmembrane receptor have shown that mutations of proline residues embedded in transmembrane regions can have a deleterious effect on the kinetics and robustness of folding.[33]

4.1.6 Substitution at 301

In all, 13 different amino acids were incorporated at position 301, and much like with 308, only six produced functional receptors (see Table 4.3). In contrast to the substitution pattern at 308, however, residues not maintaining a cyclic structure produced functional receptors at 301. The dose-response data show that none of the functional mutations lead to large changes in EC_{50}. (Figure 4.11 and Table 4.3) Substitution by Val resulted in a 3-fold decrease in EC_{50}. The fact, that this standard residue which has a hydrogen at the amide position and shows a strong preference for the *trans*-amide

produced functional receptors with only a modest shift in EC_{50} indicates that neither the special hydrogen-bonding properties of proline nor a *cis*-proline are important at this site. Incorporation of Vah, dmP, and Pip at 301 lead to roughly 2-fold increases in EC_{50}, and incorporation of Aze lead to a 2-fold decrease in EC_{50}. Thus, aside from the Val mutations, the dose-response data do not point to any special features of this site.

All functional mutations, however, did lead to increases in the macroscopic rates of activation and deactivation (Figure 4.12 and Table 4.3). Val, Aze and Pip resulted in 3- to 4-fold increases in the activation rates and 9- to 14-fold increases in deactivation rates. More dramatic rate increases were seen with dmP and Vah. The former lead to 22- and 68-fold increases in activation and deactivation, respectively, and the latter lead to 25- and 85-fold increases in activation and deactivation, respectively. The only obvious parallels between the two residues is that relative to proline and the other mutations, both dmP and Vah have lower barriers for amide bond isomerization. The results for Val, however, make this a doubtful scenario. Thus, position 301 does seem to be tuned for the presence of proline, as all mutations were either non-functional or lead to rate increases. Given that the cryo-EM structure of the transmembrane domains shows a kink in the helix at Pro 265 (the homolog of 301), it seems possible that this proline may establish the proper orientation of the M2 helix. Thus, the changes we observe in the rates may reflect alterations in the M2 helix kink and/or orientation.

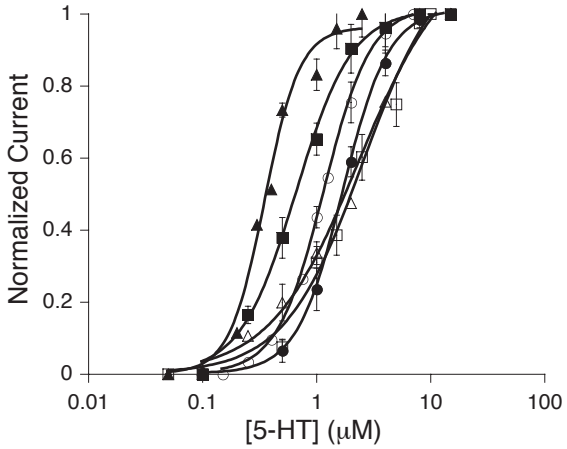

Figure 4.11. Dose-response relations for Pro 301 mutants. Pro (*open circles*), Aze (*filled squares*), Pip (*filled circles*), dmP (*open triangles*), Val (*filled triangles*), and Vah (*open squares*).

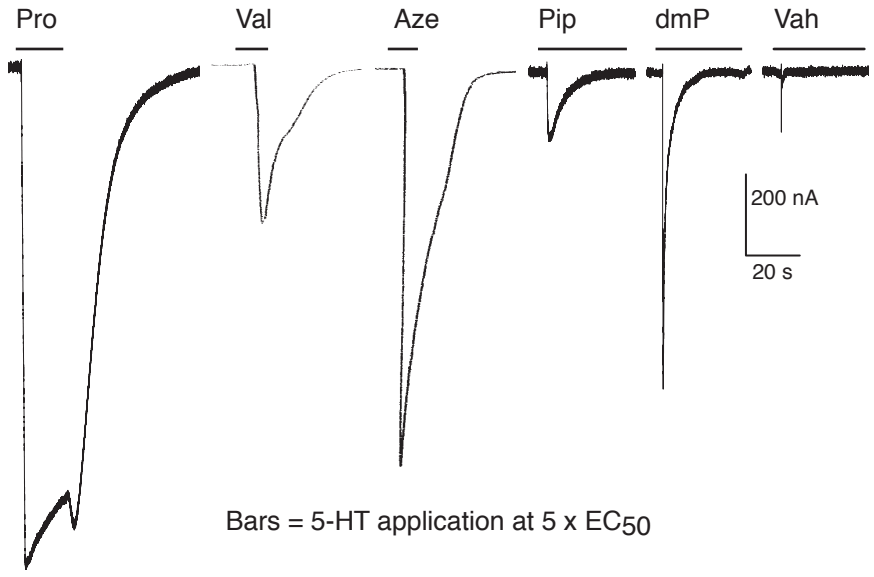

Figure 4.12. Current traces showing the altered rates of activation and deactivation for the 301 mutants. Bars represent application of 5-HT at 5 times EC_{50} of the respective mutant.

Table 4.3 Dose-response data and macroscopic rates for the Pro 301 mutants

Residue	EC_{50}±SEM (μM)	Hill±SEM	Act. rate±SEM (s^{-1})	Deact. Rate±SEM (s^{-1})
Pro	1.18 ± 0.02	2.12 ± 0.08	2.85 ± 0.91	0.02 ± 0.0005
Aze	0.68 ± 0.03	1.77 ± 0.11	10.75 ± 2.64	0.16 ± 0.021
Pip	1.73 ± 0.02	2.16 ± 0.04	12.45 ± 2.94	0.25 ± 0.026
Val	0.36 ± 0.02	2.82 ± 0.47	9.62 ± 2.07	0.13 ± 0.022
Vah	2.6 ± 0.62	1.27 ± 0.22	71.11 ± 5.66	1.46 ± 0.013
dmP	2.37 ± 0.54	1.12 ± 0.17	64.44 ± 4.48	1.15 ± 0.101
Ala	NR	NR		
Gly	NR	NR		
Sar	NR	NR		
NMeLeu	NR	NR		
*trans*3MePro	NR	NR		
2,4MPro	NR	NR		
2MePro	NR	NR		

NR = no response to concentrations up to 1 mM 5-HT

4.6 Discussion

Agonist binding in ligand-gated ion channels initiates a series of conformational changes that ultimately lead to opening of an ion permeant channel across the cell membrane. The molecular details linking binding to the channel gate some 50 Å away remain largely unknown. From a chemical standpoint, this is an intriguing consideration: how does the noncovalent binding of a small molecule induce a dramatic structural change in a multisubunit ~300 kDa protein?

Previous work has indicated a potentially prominent role for the M2-M3 loop in the gating pathway. This small loop connects the channel-lining domain (M2) with the M3 domain, and is an appealing candidate because of its location at the interface between the binding and transmembrane domains (Figure 4.1). To investigate the functional role of the M2-M3 loop, we have probed two conserved prolines in this domain using unnatural amino acids. Our findings indicate Pro 301 and Pro 308 are functionally important in the

gating pathway, and in particular the results at Pro 308 lend experimental support for a recently proposed gating model

Based on cryo-EM data from the nAChR, the model posits that binding of agonist induces a 15° rotation of the extracellular domains.[6] This rotation leads to contact between the β1-β2 loop of the extracellular domain and the M2-M3 loop. Specifically, Val 44 docks into a hydrophobic pocket formed by Ser269-Pro 272. This then provides the torsional force for movement of the M2 domain and gating of the channel. In the model, the M2-M3 loop not only acts as the mechanical receiver of conformational changes in the extracellular domain, but also serves as the hinge for the gating movement of M2. Pro 308 in the 5-HT_3R aligns with Pro 272 of the nAChR. This residue is conserved amongst the cation-selective members of the Cys-loop family. Our data support a conformational change at Pro 308 during the gating process that is consistent with this domain functioning as a hinge.

The data show that Pro 308 is a highly stringent site that requires a rigid ring structure for proper receptor function. Substitution by Ala, Gly, Sar, Val, Vah or N-Me-Leu resulted in receptors that were expressed at the cell surface, but did not respond to agonist, indicating these mutations decoupled agonist binding and channel gating. A rigid ring structure, however, is not sufficient. Substitution by *trans*-3-Me-Pro, 2-Me-Pro, or 2,4MPro also leads to surfaced-expressed, yet nonfunctional receptors (Figure 4.10). This group of mutations shares a common characteristic in that they disfavor the *cis*-amide isomer. In model peptide studies, 2-Me-Pro and 2,4-methano-Pro showed no detectable *cis* isomer, and *trans*-3-Me-Pro has a higher barrier to

isomerization relative to proline.[44, 49, 54] These results suggest the possibility that a *cis*-peptide bond is functionally important at Pro 308.

This conclusion is supported by the dose-response data, where incorporation of the *cis*-selective proline analog, dmP leads to a significant decrease in EC_{50}. Furthermore a plot of $\Delta\Delta G$ EC_{50} for the various mutants versus the $\Delta\Delta G$ values for the *cis* preference of the analogs relative to proline shows a linear correlation (Figure 4.6). The correlation between EC_{50} and *cis* preference is seen for over two-orders of magnitude change in EC_{50} and almost a 2.5 kcal difference in *cis* preference. This is fairly compelling evidence for a functionally important *cis*-proline at 308.

It is also possible that given the increased steric bulk of dmP, this residue is altering the conformation of the M2-M3 loop in a way that biases the receptor towards the open state. The functional role of Pro 308, however, does appear to be dynamic, as activation of the dmP mutants lead to an increase in the standing current that was blockable by TMB-8 (Figure 4.7). This standing current was seen only after initial activation of the mutant receptors and grew progressively larger after each application of 5-HT. This seems to indicate that once open the dmP mutant is slow to deactivate (i.e. transiting to either the desensitized or closed state). This result suggests that the gating process involves a conformational change at Pro 308. A consistent interpretation of this finding combined with the immunofluorescence and dose-response data is that in the resting closed state, Pro 308 is in the *trans*-conformation and during gating, it isomerizes to the *cis*-conformation (Figure 4.13). It is also possible that the functional changes we see with the 308 mutants reflect a gating specific heterogeneity in the conformation of Pro 308 that does not involve *cis*/*trans* isomerization. Pro 308 may function as a

conformational switch converting between two stable orientations of ψ. Our findings, however, do support a dynamic role for Pro 308 in the gating pathway.

The results at Pro 301 are also suggestive of a role in the gating pathway. Here, however, we did not see large changes in EC_{50}, but changes in the macroscopic rates. This site is not as stringent as Pro 308 and the data do not suggest any obvious trend, as both cyclic proline analogs, natural amino acids and the hydroxy acid Vah lead to functional receptors. The rate changes however suggest that indeed, the mutations were affecting the gating pathway, possibly by changing the orientation or kink angle of the M2 helix.

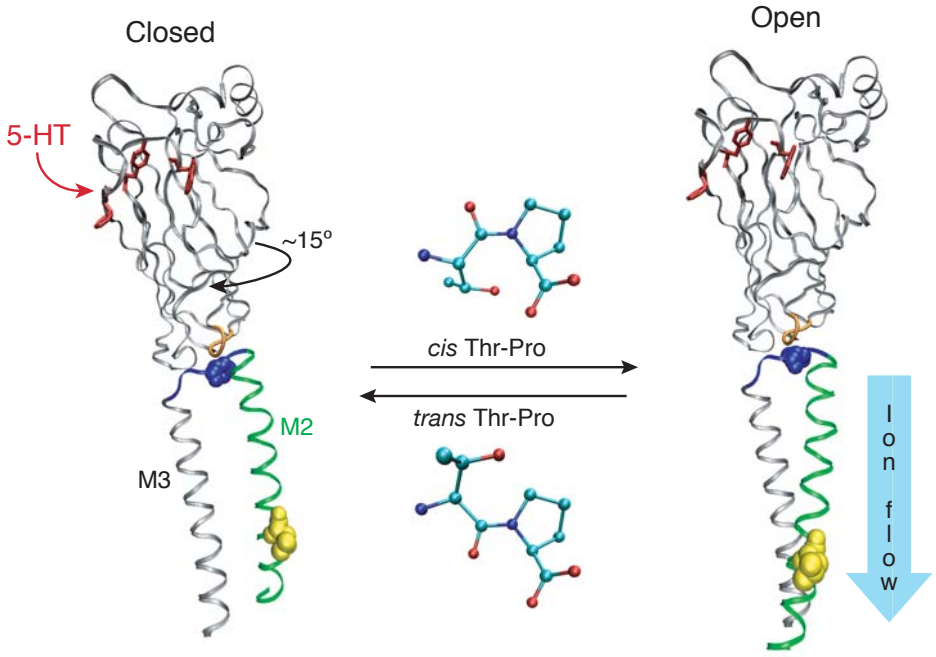

Figure 4.13. Cartoon of a single 5-HT_3R subunit depicting how *trans* to *cis* isomerization could function as a hinge for movement of M2 (green) during gating. The general gating mechanism is based on Unwin's proposed model, where agonist binding (red) induces a rotation of the extracellular domains. This brings the β1-β2 loop (orange) into contact with the M2-M3 loop (blue) causing the latter loop to pivot. Here the pivot is depicted as *trans* to *cis* isomerization of Pro 308 (blue CPK). The hinge movement in the M2-M3 loop allows rotation of M2 and gates the channel. Leu 9', the gate, is shown in yellow CPK. The open structure on the right was generated by manually converting Pro 308 to the *cis* conformation.

4.7 Future directions

In conclusion, our findings support a functional role for both Pro 301 and Pro 308 in the gating process of the 5-HT_3R. The results at Pro 308 in particular suggest this site functions as a conformational switch during gating, which is consistent with Unwin's prediction that the M2-M3 loop serves as a hinge during the gating process. Several possibilities, however, could be pursued to strengthen this conclusion. First, the plot of $\Delta\Delta G$ EC_{50} versus $\Delta\Delta G$ *cis* preference requires an intermediate data point between dmP and Aze. Experiments by Lori Lee with *cis*-5-*tBu*-Pro are currently underway to remedy this concern. Second, if Pro 308 does indeed function as a conformational switch (either through *cis*/*trans* isomerization or converting between stable ψ conformations) this is likely to be a mechanism that is at least conserved in the nAChR, which also has a proline at this site. Thus, repeating these studies in the nAChR is a necessary validation of our conclusions. And third, for both the 301 and 308 studies the nAChR offers the possibility to combine unnatural mutagenesis with single–channel experiments. This would allow better resolution of the mutational effects, and could provide telling information on how these mutations perturb the gating mechanism.

4.8 Methods

4.8.1 Synthesis of dCA-NVOC-5,5-dimethylproline

Synthesis of NVOC-DL-5,5-dimethylproline was adapted from the procedure of Magaard and coworkers[64] (Scheme 4.1).

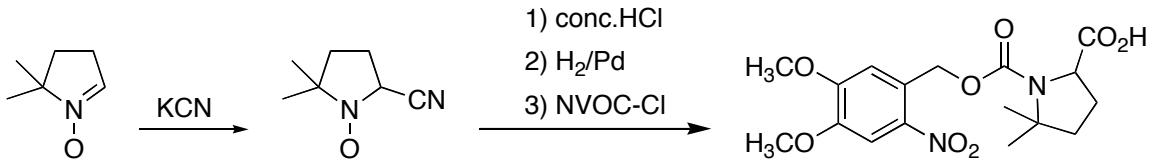

Scheme 4.1 Adapted synthesis of NVOC-DL-5,5-dimethylproline.

4.8.1.1 1-Hydroxy-2-cyano-5,5-dimethylpyrrolidine

KCN (1.15 g, 17.6 mmol) was dissolved in 2.5 mL of water and cooled to –10° C. To this was added 5,5-dimethyl-1-pyrroline N-oxide (1 g, 8.8 mmol) in 2.5 mL of water. 2 N HCl (25 mL) was added dropwise over one hour, then stirred at 0° C for 3 hours and at room temperature overnight. The pH was adjusted to 11 with 6 N KOH and the solution was extracted with diethyl ether. The ether extracts were dried over $MgSO_4$ and rotary evaporated to yield 0.92 g (75% yield) of a white powder. ^{1}H NMR (300 MHz, $CDCl_3$) δ = 1.06 (6H, s), 1.67-1.84 (2H, m), 1.99-2.28 (2H, m), 3.92 (1H, t), 6.25 (1H, s). ^{13}C NMR (75 MHz, $CDCl_3$) δ = 19.4, 34.4, 54.8, 64.4, 120.5. MS Calcd for $C_7H_{11}N_2O$ 139.18. Found: (ESI^+) 141.0 $[M+H^+]^+$.

4.1.1.2 NVOC-DL-5,5-dimethylproline

1-Hydroxy-2-cyano-5,5-dimethylpyrrolidine (400 mg, 2.8 mmol) was hydrolyzed in conc. HCl (1.6 mL) at 50° C for 5 hours and evaporated to a white solid. After evaporating from water two times to remove traces of HCl, the residue was dissolved in 20 mL of methanol/water 1:1 and hydrogenated over 10% Pd/C (120 mg) at 1 atm for 4 hours. The reaction was filtered through celite to remove the catalyst and the solvent was removed by rotary evaporation. The product was then dissolved in 25 mL of water/dioxane 1:1 and Na_2CO_3 (742 mg, 7 mmol) was added. A solution of NVOC-Cl (1.1 g, 3.9 mmol) in 25 mL water/dioxane was added dropwise and the mixture was

allowed to stir. After two hours, 50 mL of CH_2Cl_2 was added followed by 1 M (aq) $KHSO_4$ (25 mL). The aqueous layer was extracted three times with 25 mL CH_2Cl_2. The organic extracts were combined, dried over $MgSO_4$, and the solvent was removed by rotary evaporation. The crude product was purified by flash chromatography (silica, 50:50 hexane/ethyl acetate w/ 1% acetic acid) to give a bright orange solid (210 mg, 20% yield). ^{1}H NMR (300 MHz, $CDCl_3$) δ = 1.40 (3H, s), 1.56 (3H, s), 1.79-2.08 (3H, m), 2.08-2.32 (1H, m), 3.91 (3H, s), 3.94 (3H, s), 4.50-4.56 (1H, m), 5.45 (2H, dd), 6.94 (1H, s), 7.65 (1H, s). ^{13}C NMR (75 MHz, $CDCl_3$) δ = 25.3, 26.3,26.6, 39.5, 56.3, 56.5, 60.8, 61.8, 64.1, 107.9, 109.2, 128.2, 140.4, 147.7, 153.8, 155.1, 178.1. MS Calcd for $C_{17}H_{22}N_2O_8$ 382.37. Found: (ESI$^-$) 381.2 $[M-H]^-$.

4.1.1.3 NVOC-DL-5,5-dimethylproline cyanomethyl ester

Under positive argon pressure, a dried flask was charged with a solution of NVOC-5,5-dimethylproline (75 mg, 0.19 mmol) dissolved in 3 mL of dry DMF. Triethylamine (66 μL, 0.48 mmol) and $ClCH_2CN$ (3 mL, 47 mmol) were added; the reaction was run under a continuous stream of argon. After six hours, the volatiles were removed *in vacuo* and the crude product was purified by flash chromatography (silica, 3/1/hexane/ethyl acetate) to give an orange oil (0.63 mg, 80% yield). ^{1}H NMR (300 MHz, $CDCl_3$) δ = 1.41 (3H, s), 1.57 (3H, s), 1.85-2.04 (3H, m), 2.22-2.38 (1H, m), 3.94 (3H, s) 4.0 (3H, s), 4.54-4.58 (1H, m), 4.76 (2H, q), 5.51 (2H, dd), 6.93 (1H, s), 7.69 (1H, s). ^{13}C NMR (75 MHz, $CDCl_3$) δ = 25.4, 26.4, 27.1, 39.4, 48.9, 56.4, 56.5, 60.5, 61.8, 64.2, 108.2, 109.9, 114.0, 128.3, 139.4, 148.0, 152.3, 153.8, 171.3. MS Calcd for $C_{19}H_{23}N_3O_8$ 421.4. Found: (ESI$^+$) 422.0 $[M+H^+]^+$.

4.1.1.4 dCA-NVOC-DL-5,5-dimethylproline

To a dry flask was added NVOC-5,5-dimethylproline cyanomethyl ester (25 mg, 0.06 mmol), dCA (20 mg), and 0.8 mL of dry DMF, and the reaction was stirred under argon. The reaction was monitored by reverse-phase HPLC. After four hours, the reaction was purified by semi-preparative reverse phase (C_{18}) HPLC. The appropriate fractions were combined and lyophilized. The white powder was dissolved in 10 mM acetic acid and lyophilized. This step was repeated to yield a white fluffy powder (3.3 mg). MS Calcd for $C_{36}H_{45}N_{10}O_{21}P_2$ 1016.75. Found: (ESI^+) 1017.8 $[M+H^+]^+$.

4.1.2 Mutagenesis and preparation of cRNA and Oocytes

Mutant 5-HT_{3A} receptor subunits were developed using the eukaryotic expression vector pcDNA 3.1 (InVitrogen, Abingdon, U.K.) containing the complete coding sequence for the 5-$HT_{3A(b)}$ subunit from NIE-115 cells as previously described.[65] Mutagenesis reactions were performed using the Kunkel method[66], and confirmed by DNA sequencing. Wild type and mutant receptor subunit coding sequences were then subcloned into pGEMHE plasmid.[67] This was linearized with Nhe1 (New England Biolabs) and cRNA synthesized using T7 mMESSAGE mMACHINE kit (Ambion). Oocytes from Xenopus laevis were prepared and maintained according to standard laboratory protocol.

4.1.3 Synthesis of tRNA and dCA-amino acids

Unnatural amino acids were chemically synthesized as nitroveratryloxycarbonyl (NVOC) protected cyanomethyl esters and coupled to the dinucleotide dCA, which was then enzymatically ligated to 74-mer THG73 $tRNA_{CUA}$ as detailed previously [68].

Immediately prior to co-injection with mRNA, tRNA-aa was deprotected by photolysis [69]. Typically, 5 ng mRNA and 25 ng tRNA-aa were injected into Stage V-VI oocytes in a total volume of 50 nl. For control experiments, mRNA was injected 1) in the absence of tRNA and 2) with the THG73 74-mer tRNA. Electrophysiological experiments were performed 18 to 36 hours post injection.

4.1.4 Characterization of mutant receptors

5-HT-induced currents were recorded from individual oocytes using two-electrode voltage clamp with either a GeneClamp 500 amplifier or an OpusXpress system (Axon Instruments, Inc., Union City, CA). All experiments were performed at 22-25º C. Serotonin (creatinine sulphate complex, Sigma) was stored as 25 mM aliquots at –80°C, diluted in calcium-free ND96, and delivered to cells via computer-controlled perfusion systems. Glass microelectrodes were backfilled with 3 M KCl and had a resistance of approximately 1 MΩ. The holding potential was –60 mV unless otherwise specified. To determine EC_{50}s, 5-HT concentration-response data were fitted to the Hill equation, $I = (I_{max}[A]^n)/(EC_{50}{}^n + [A]^n)$,where I_{max} is the maximal peak current, [*A*] is the concentration of agonist, and n is the Hill coefficient.

4.9 References

1. Lummis, S. C. R., The transmembrane domain of the 5-HT3 receptor: its role in selectivity and gating. *Biochemical Society Transactions* **2004,** 32, 535-539.
2. Absalom, N. L.; Lewis, T. M.; Schofield, P. R., Mechanisms of channel gating of the ligand-gated ion channel superfamily inferred from protein structure. *Experimental Physiology* **2004,** 89, (2), 145-153.
3. Lester, H. A.; Dibas, M. I.; Dahan, D. S.; Leite, J. F.; Dougherty, D. A., Cys-loop receptors: new twists and turns. *Trends in Neurosciences* **2004,** 27, (6), 329-336.
4. Brejc, K.; van Dijk, W. J.; Klaassen, R. V.; Schuurmans, M.; van der Oost, J.; Smit, A. B.; Sixma, T. K., Crystal structure of an ACh-binding protein reveals the ligand-binding domain of nicotinic receptors. *Nature* **2001,** 411, (6835), 269-276.
5. Celie, P. H. N.; van Rossum-Fikkert, S. E.; van Dijk, W. J.; Brejc, K.; Smit, A. B.; Sixma, T. K., Nicotine and carbamylcholine binding to nicotinic acetylcholine receptors as studied in AChBP crystal structures. *Neuron* **2004,** 41, (6), 907-914.

6. Miyazawa, A.; Fujiyoshi, Y.; Unwin, N., Structure and gating mechanism of the acetylcholine receptor pore. *Nature* **2003,** 423, (6943), 949-955.
7. Dougherty, D. A.; Lester, H. A., Neurobiology - Snails, synapses and smokers. *Nature* **2001,** 411, (6835), 252-254.
8. Kash, T. L.; Jenkins, A.; Kelley, J. C.; Trudell, J. R.; Harrison, N. L., Coupling of agonist binding to channel gating in the GABA(A) receptor. *Nature* **2003,** 421, (6920), 272-275.
9. Bouzat, C.; Gumilar, F.; Spitzmaul, G.; Wang, H. L.; Rayes, D.; Hansen, S. B.; Taylor, P.; Sine, S. M., Coupling of agonist binding to channel gating in an ACh-binding protein linked to an ion channel. *Nature* **2004,** 430, (7002), 896-900.
10. Absalom, N. L.; Lewis, T. M.; Kaplan, W.; Pierce, K. D.; Schofield, P. R., Role of charged residues in coupling ligand binding and channel activation in the extracellular domain of the glycine receptor. *Journal of Biological Chemistry* **2003,** 278, (50), 50151-50157.
11. Beckstein, O., Tai, K., and Sansom, M.P., Not Ions Alone: Barriers to Ion Permeation in Nanopores and Channels. *Journal of the American Chemical Society* **2004,** 126, (45), 14695-14696.
12. Reeves, D. C.; Goren, E. N.; Akabas, M. H.; Lummis, S. C. R., Structural and electrostatic properties of the 5-HT3 receptor pore revealed by substituted cysteine accessibility mutagenesis. *Journal of Biological Chemistry* **2001,** 276, (45), 42035-42042.
13. Akabas, M. H.; Kaufmann, C.; Archdeacon, P.; Karlin, A., Identification of Acetylcholine-Receptor Channel-Lining Residues in the Entire M2 Segment of the Alpha-Subunit. *Neuron* **1994,** 13, (4), 919-927.
14. Unwin, N., Nicotinic Acetylcholine-Receptor at 9-Angstrom Resolution. *Journal of Molecular Biology* **1993,** 229, (4), 1101-1124.
15. Labarca, C.; Nowak, M. W.; Zhang, H.; Tang, L.; Deshpande, P.; Lester, H. A., Channel gating governed symmetrically by conserved leucine residues in the M2 domain of nicotinic receptors. *Nature* **1995,** 376, (6540), 514-6.
16. Bera, A. K.; Chatav, M.; Akabas, M. H., GABA(A) receptor M2-M3 loop secondary structure and changes in accessibility during channel gating. *Journal of Biological Chemistry* **2002,** 277, (45), 43002-43010.
17. Wick, M. J.; Mihic, S. J.; Ueno, S.; Mascia, M. P.; Trudell, J. R.; Brozowski, S. J.; Ye, Q.; Harrison, N. L.; Harris, R. A., Mutations of gamma-aminobutyric acid and glycine receptors change alcohol cutoff: Evidence for an alcohol receptor? *Proceedings of the National Academy of Sciences of the United States of America* **1998,** 95, (11), 6504-6509.
18. Rovira, J. C.; Ballesta, J. J.; Vicente-Agullo, F.; Campos-Caro, A.; Criado, M.; Sala, F.; Sala, S., A residue in the middle of the M2-M3 loop of the beta(4) subunit specifically affects gating of neuronal nicotinic receptors. *Febs Letters* **1998,** 433, (1-2), 89-92.
19. Rovira, J. C.; Vicente-Agullo, F.; Campos-Caro, A.; Criado, M.; Sala, F.; Sala, S.; Ballesta, J. J., Gating of alpha(3)beta(4) neuronal nicotinic receptor can be controlled by the loop M2-M3 of both alpha(3) and beta(4) subunits. *Pflugers Archiv-European Journal of Physiology* **1999,** 439, (1-2), 86-92.
20. Lynch, J. W.; Rajendra, S.; Pierce, K. D.; Handford, C. A.; Barry, P. H.; Schofield, P. R., Identification of intracellular and extracellular domains mediating signal transduction in the inhibitory glycine receptor chloride channel. *Embo Journal* **1997,** 16, (1), 110-120.
21. Lynch, J. W.; Rajendra, S.; Barry, P. H.; Schofield, P. R., Mutations Affecting the Glycine Receptor Agonist Transduction Mechanism Convert the Competitive Antagonist, Picrotoxin, into an Allosteric Potentiator. *Journal of Biological Chemistry* **1995,** 270, (23), 13799-13806.
22. CamposCaro, A.; Sala, S.; Ballesta, J. J.; VicenteAgullo, F.; Criado, M.; Sala, F., A single residue in the M2-M3 loop is a major determinant of coupling between binding and gating in neuronal nicotinic receptors. *Proceedings of the National Academy of Sciences of the United States of America* **1996,** 93, (12), 6118-6123.
23. Grosman, C.; Salamone, F. N.; Sine, S. M.; Auerbach, A., The extracellular linker of muscle acetylcholine receptor channels is a gating control element. *Journal of General Physiology* **2000,** 116, (3), 327-339.
24. Lynch, J. W.; Han, N. L. R.; Haddrill, J.; Pierce, K. D.; Schofield, P. R., The surface accessibility of the glycine receptor M2-M3 loop is increased in the channel open state. *Journal of Neuroscience* **2001,** 21, (8), 2589-2599.
25. Macarthur, M. W.; Thornton, J. M., Influence of Proline Residues on Protein Conformation. *Journal of Molecular Biology* **1991,** 218, (2), 397-412.

26. Chakrabarti, P.; Pal, D., The interrelationships of side-chain and main-chain conformations in proteins. *Progress in Biophysics & Molecular Biology* **2001,** 76, (1-2), 1-102.
27. Brandl, C. J.; Deber, C. M., Hypothesis About the Function of Membrane-Buried Proline Residues in Transport Proteins. *Proceedings of the National Academy of Sciences of the United States of America* **1986,** 83, (4), 917-921.
28. Sansom, M. S. P.; Weinstein, H., Hinges, swivels and switches: the role of prolines in signalling via transmembrane alpha-helices. *Trends in Pharmacological Sciences* **2000,** 21, (11), 445-451.
29. Tieleman, D. P.; Shrivastava, I. H.; Ulmschneider, M. R.; Sansom, M. S. P., Proline-induced hinges in transmembrane helices: Possible roles in ion channel gating. *Proteins-Structure Function and Genetics* **2001,** 44, (2), 63-72.
30. Williams, K. A.; Deber, C. M., Proline Residues in Transmembrane Helices - Structural or Dynamic Role. *Biochemistry* **1991,** 30, (37), 8919-8923.
31. Partridge, A. W.; Therien, A. G.; Deber, C. M., Missense mutations in transmembrane domains of proteins: Phenotypic propensity of polar residues for human disease. *Proteins-Structure Function and Bioinformatics* **2004,** 54, (4), 648-656.
32. Sankararamakrishnan, R.; Vishveshwara, S., Geometry of Proline-Containing Alpha-Helices in Proteins. *International Journal of Peptide and Protein Research* **1992,** 39, (4), 356-363.
33. Senes, A.; Engel, D. E.; DeGrado, W. F., Folding of helical membrane proteins: the role of polar, GxxxG-like and proline motifs. *Current Opinion in Structural Biology* **2004,** 14, (4), 465-479.
34. Deber, C. M.; Glibowicka, M.; Woolley, G. A., Conformations of Proline Residues in Membrane Environments. *Biopolymers* **1990,** 29, (1), 149-157.
35. Deane, C. M.; Lummis, S. C. R., The role and predicted propensity of conserved proline residues in the 5-HT3 receptor. *Journal of Biological Chemistry* **2001,** 276, (41), 37962-37966.
36. Pal, D.; Chakrabarti, P., Cis peptide bonds in proteins: Residues involved, their conformations, interactions and locations. *Journal of Molecular Biology* **1999,** 294, (1), 271-288.
37. Bhattacharyya, R.; Chakrabarti, P., Stereospecific interactions of proline residues in protein structures and complexes. *Journal of Molecular Biology* **2003,** 331, (4), 925-940.
38. Andreotti, A. H., Native state proline isomerization: An intrinsic molecular switch. *Biochemistry* **2003,** 42, (32), 9515-9524.
39. Mallis, R. J.; Brazin, K. N.; Fulton, D. B.; Andreotti, A. H., Structural characterization of a proline-driven conformational switch within the Itk SH2 domain. *Nature Structural Biology* **2002,** 9, (12), 900-905.
40. Martin, A.; Schmid, F. X., A proline switch controls folding and domain interactions in the gene-3-protein of the filamentous phage fd. *Journal of Molecular Biology* **2003,** 331, (5), 1131-1140.
41. Gitti, R. K.; Lee, B. M.; Walker, J.; Summers, M. F.; Yoo, S.; Sundquist, W. I., Structure of the amino-terminal core domain of the HIV-1 capsid protein. *Science* **1996,** 273, (5272), 231-235.
42. Suchyna, T. M.; Xu, L. X.; Gao, F.; Fourtner, C. R.; Nicholson, B. J., Identification of a Proline Residue as a Transduction Element Involved in Voltage Gating of Gap-Junctions. *Nature* **1993,** 365, (6449), 847-849.
43. Demene, H.; Granier, S.; Muller, D.; Guillon, G.; Dufour, M. N.; Delsuc, M. A.; Hibert, M.; Pascal, R.; Mendre, C., Active peptidic mimics of the second intracellular loop of the V-1A vasopressin receptor are structurally related to the second intracellular rhodopsin loop: A combined H-1 NMR and biochemical study. *Biochemistry* **2003,** 42, (27), 8204-8213.
44. Beausoleil, E.; Sharma, R.; Michnick, S. W.; Lubell, W. D., Alkyl 3-position substituents retard the isomerization of prolyl and hydroxyprolyl amides in water. *Journal of Organic Chemistry* **1998,** 63, (19), 6572-6578.
45. Dugave, C.; Demange, L., Cis-trans isomerization of organic molecules and biomolecules: Implications and applications. *Chemical Reviews* **2003,** 103, (7), 2475-2532.
46. Kern, D.; Schutkowski, M.; Drakenberg, T., Rotational barriers of cis/trans isomerization of proline analogues and their catalysis by cyclophilin. *Journal of the American Chemical Society* **1997,** 119, (36), 8403-8408.
47. Renner, C.; Alefelder, S.; Bae, J. H.; Budisa, N.; Huber, R.; Moroder, L., Fluoroprolines as tools for protein design and engineering. *Angewandte Chemie-International Edition* **2001,** 40, (5), 923-925.
48. An, S. S. A.; Lester, C. C.; Peng, J. L.; Li, Y. J.; Rothwarf, D. M.; Welker, E.; Thannhauser, T. W.; Zhang, L. S.; Tam, J. P.; Scheraga, H. A., Retention of the cis proline conformation in tripeptide fragments of bovine pancreatic ribonuclease A containing a non-natural proline analogue, 5,5-dimethylproline. *Journal of the American Chemical Society* **1999,** 121, (49), 11558-11566.

49. Delaney, N. G.; Madison, V., Novel Conformational Distributions of Methylproline Peptides. *Journal of the American Chemical Society* **1982,** 104, (24), 6635-6641.
50. Hunston, R. N.; Gerothanassis, I. P.; Lauterwein, J., A Study of L-Proline, Sarcosine, and the Cis Trans Isomers of N-Acetyl-L-Proline and N-Acetylsarcosine in Aqueous and Organic Solution by O-17 Nmr. *Journal of the American Chemical Society* **1985,** 107, (9), 2654-2661.
51. Dang, H.; England, P. M.; Farivar, S. S.; Dougherty, D. A.; Lester, H. A., Probing the role of a conserved M1 proline residue in 5-hydroxytryptamine(3) receptor gating. *Molecular Pharmacology* **2000,** 57, (6), 1114-1122.
52. England, P. M.; Zhang, Y. N.; Dougherty, D. A.; Lester, H. A., Backbone mutations in transmembrane domains of a ligand-gated ion channel: Implications for the mechanism of gating. *Cell* **1999,** 96, (1), 89-98.
53. Improta, R.; Benzi, C.; Barone, V., Understanding the role of stereoelectronic effects in determining collagen stability. 1. A quantum mechanical study of proline, hydroxyproline, and fluoroproline dipeptide analogues in aqueous solution. *Journal of the American Chemical Society* **2001,** 123, (50), 12568-12577.
54. Matsui, S.; Srivastava, V. P.; Holt, E. M.; Taylor, E. W.; Stammer, C. H., Synthesis and Conformational-Analysis of L-Aspartylproline and L-Aspartyl-2,3-Methanoproline Propyl Esters. *International Journal of Peptide and Protein Research* **1991,** 37, (4), 306-314.
55. Nowak, M. W.; Gallivan, J. P.; Silverman, S. K.; Labarca, C. G.; Dougherty, D. A.; Lester, H. A., In vivo incorporation of unnatural amino acids into ion channels in Xenopus oocyte expression system. *Methods in Enzymology* **1998,** 293, 504-529.
56. Reimer, U.; Fischer, G., Local structural changes caused by peptidyl-prolyl cis/trans isomerization in the native state of proteins. *Biophysical Chemistry* **2002,** 96, (2-3), 203-212.
57. Milnerwhite, E. J.; Bell, L. H.; Maccallum, P. H., Pyrrolidine Ring Puckering in Cis and Trans-Proline Residues in Proteins and Polypeptides - Different Puckers Are Favored in Certain Situations. *Journal of Molecular Biology* **1992,** 228, (3), 725-734.
58. DeRider, M. L.; Wilkens, S. J.; Waddell, M. J.; Bretscher, L. E.; Weinhold, F.; Raines, R. T.; Markley, J. L., Collagen stability: Insights from NMR spectroscopic and hybrid density functional computational investigations of the effect of electronegative substituents on prolyl ring conformations. *Journal of the American Chemical Society* **2002,** 124, (11), 2497-2505.
59. Petersson, E. J.; Shahgholi, M.; Lester, H. A.; Dougherty, D. A., MALDI-TOF mass spectrometry methods for evaluation of in vitro aminoacyl tRNA production. *Rna-a Publication of the Rna Society* **2002,** 8, (4), 542-547.
60. Spier, A. D.; Wotherspoon, G.; Nayak, S. V.; Nichols, R. A.; Priestley, J. V.; Lummis, S. C. R., Antibodies against the extracellular domain of the 5-HT3 receptor label both native and recombinant receptors. *Molecular Brain Research* **1999,** 67, (2), 221-230.
61. Cox, C.; Lectka, T., Intramolecular catalysis of amide isomerization: Kinetic consequences of the 5-NH- -N-a hydrogen bond in prolyl peptides. *Journal of the American Chemical Society* **1998,** 120, (41), 10660-10668.
62. Rankin, K. N.; Boyd, R. J., A computational study of the isomerization of prolyl amides as catalyzed by intramolecular hydrogen bonding. *Journal of Physical Chemistry A* **2002,** 106, (46), 11168-11172.
63. Helekar, S. A.; Patrick, J., Peptidyl prolyl cis-trans isomerase activity of cyclophilin A in functional homo-oligomeric receptor expression. *Proceedings of the National Academy of Sciences of the United States of America* **1997,** 94, (10), 5432-5437.
64. Magaard, V. W.; Sanchez, R. M.; Bean, J. W.; Moore, M. L., A Convenient Synthesis of the Conformationally Constrained Amino-Acid 5,5-Dimethylproline. *Tetrahedron Letters* **1993,** 34, (3), 381-384.
65. Hargreaves, A. C.; Gunthorpe, M. J.; Taylor, C. W.; Lummis, S. C. R., Direct inhibition of 5-hydroxytryptamine(3) receptors by antagonists of L-type Ca2+ channels. *Molecular Pharmacology* **1996,** 50, (5), 1284-1294.
66. Kunkel, T. A., Rapid and Efficient Site-Specific Mutagenesis without Phenotypic Selection. *Proceedings of the National Academy of Sciences of the United States of America* **1985,** 82, (2), 488-492.
67. Liman, E. R.; Tytgat, J.; Hess, P., Subunit Stoichiometry of a Mammalian K+ Channel Determined by Construction of Multimeric Cdnas. *Neuron* **1992,** 9, (5), 861-871.
68. Nowak, M. W.; Gallivan, J. P.; Silverman, S. K.; Labarca, C. G.; Dougherty, D. A.; Lester, H. A., In vivo incorporation of unnatural amino acids into ion channels in Xenopus oocyte expression system. *Methods Enzymol* **1998,** 293, 504-29.

69. Kearney, P. C.; Nowak, M. W.; Zhong, W.; Silverman, S. K.; Lester, H. A.; Dougherty, D. A., Dose-response relations for unnatural amino acids at the agonist binding site of the nicotinic acetylcholine receptor: tests with novel side chains and with several agonists. *Mol Pharmacol* **1996,** 50, (5), 1401-12.